

PROJECT FINAL REPORT.....DE-FG03-94ER45510.....12/1/93 TO 2/28/97

PI: R.W.CARPENTER & S.H.LIN.....ARIZONA STATE UNIVERSITY

1. **Interface and grain boundary chemistry and structure in silicon nitride matrix/silicon carbide whisker composites, and in monolithic silicon nitride and silicon carbide synthesized by several different methods.**

Off-stoichiometric, impurity, and sintering aid elemental distributions in these materials (and other ceramics) have been of great interest because of expected effects on properties but these distributions have proven very difficult to measure because the spatial resolution required is high. We made a number of these measurements for the first time, using techniques and instrumentation developed here.

1.1. Silicon nitride matrix/silicon carbide whisker composites

We examined for the first time sintering aid distributions at whisker/matrix interfaces and matrix grain boundaries in four different $\text{Si}_3\text{N}_4/\text{SiC}(w)$ using high spatial resolution (field emission source TEM) position-resolved electron energy loss spectroscopy (PREELS), high resolution annular dark field STEM imaging (Z-contrast), energy selected TEM imaging (ESTEMI), and energy dispersive x-ray spectroscopy (EDS). These results were correlated with structure of the boundaries & interfaces observed by HRTEM imaging. A comprehensive discussion of these results is given in Das Chowdhury et al. (1995). The spectroscopic and chemically sensitive imaging methods we used showed that the sintering aids were *continuously* distributed along all matrix grain boundaries and had formed diffusion zones extending into the bounding crystals that were wider than the structural width of the boundaries determined by HRTEM. So there were two widths associated with each boundary: chemical width and structural width. SiC whisker/matrix interfaces were similar; in this case, however, the chemical widths (i.e. sintering aid distributions) were laterally discontinuous along the interfaces. This behavior was due to atomically sharp steps formed on the SiC whisker surfaces during their synthesis processes, prior to the composite synthesis. The step sharpness and heights were reduced by a Gibbs-Thompson dissolution into the liquid phase during composite densification, but remained sufficiently well defined to cause nearly point contacts that excluded the liquid densification phase at those points between the whiskers and the smooth surfaced nitride matrix grains. The primary microstructural difference among the four composites was the lateral spacing of these discontinuities, which implies that the whisker-matrix bond strength varies laterally along their interfaces. This implies that engineering mechanical properties will be affected, since interface bond strength is considered a primary variable in mechanical performance, but unambiguous direct measurements of interface bond strength have not been made.

The HRTEM structural width of both grain boundaries and whisker/ matrix interfaces varied within each composite, as well as among the four composites. The ratios of chemical to structural widths for nitride/carbide interfaces was in the range of 10 to 40, and for nitride matrix boundaries the ratios were in the range of 70 to 120. The elemental distribution plots, from which the chemical widths were determined, were in general asymmetrical about the edge-on interface/boundary planes for nitride/carbide and symmetric for nitride/nitride. In addition, the solubility of the densification aid elements added during processing is higher in the nitride than in the carbide phase. These two factors were the main reasons for the variability in width ratios. The widths we observed corresponded to calculated solute diffusion constants in the range 3×10^{-15} to 6×10^{-16} cm^2/sec , which is the approximate expected magnitude at 1780°C .

There was also an apparent increase in absolute chemical width magnitude when the structural width was large, i.e. when it included a finite width of amorphous boundary/interface phase. This is easy to visualize from a mathematical viewpoint, if one considers the structural width a reservoir for diffusion of the chemical elements in the densification aids (Al, Y, O) into the

MASTER

BE
Final

DISCLAIMER

This report was prepared as an account of work sponsored by an agency of the United States Government. Neither the United States Government nor any agency thereof, nor any of their employees, make any warranty, express or implied, or assumes any legal liability or responsibility for the accuracy, completeness, or usefulness of any information, apparatus, product, or process disclosed, or represents that its use would not infringe privately owned rights. Reference herein to any specific commercial product, process, or service by trade name, trademark, manufacturer, or otherwise does not necessarily constitute or imply its endorsement, recommendation, or favoring by the United States Government or any agency thereof. The views and opinions of authors expressed herein do not necessarily state or reflect those of the United States Government or any agency thereof.

DISCLAIMER

Portions of this document may be illegible in electronic image products. Images are produced from the best available original document.

bounding crystals, considered as semi-infinite half-spaces for reasonably large matrix grain size or whisker diameter. This relationship has not been quantified yet

Theoretical considerations based on equilibrium dispersion forces between the bounding crystals acting through the thin amorphous phase indicated that the thin amorphous phase should be thicker at matrix grain boundaries than at whisker/matrix interfaces. This does not appear to be a pronounced effect. However, other factors, such as non-equilibrium of the as-densified composite microstructures and structural order in the amorphous phase that mimics the structure of the bounding crystals where the amorphous phase joins a bounding crystal will moderate this effect. These important effects remain to be evaluated, using special specimens and experimental methods.

Other information about this important material system is given in the following references. Carpenter et al. (1995a, 1995b, 1994), Das Chowdhury et al. (1993a), and Liu (1993).

1.2. High purity chemical vapor deposited (CVD) silicon nitride.

Grain boundaries in polycrystalline CVD Si_3N_4 have narrow structural width ($\sim 3 \text{ \AA}$ max), with no impurity segregation detectable by EELS or EDS (Das Chowdhury et al., 1993a). The appearance of these boundaries in HRTEM images is very similar to clean grain boundaries in metals, with no trace of an amorphous phase visible. All other types of Si_3N_4 we have examined were densified using sintering aids of one type or another, and all of them exhibited chemical widths larger than the corresponding structural widths, even when the amorphous boundary phase thickness was vanishingly small, i.e. with minimum sintering aid additions.

1.3. Silicon Carbide.

High purity CVD polycrystalline SiC (obtained from Synterials Inc.) did not have any detectable impurity segregation in grain boundaries. The structural width of CVD SiC grain boundaries was also $\sim 3 \text{ \AA}$, approximately the characteristic size of a tetrahedral unit in all the Si-based ceramics we have examined. The appearance of these boundaries was very similar to the CVD Si_3N_4 and clean metal boundaries we have examined.

In monolithic SiC densified by several currently used processes, only the hot-isostatically-pressed (HIPed) material with 0.2 wt.% Al added as a densification aid exhibited a very small amount of oxygen segregation to grain boundaries (Braue et al., 1994). However, in this material as well as sintered α -SiC (with 2 wt.% B + 2 wt.% C added as densification aids) and reaction-bonded SiC (RB-SiC containing excess Si) most of the oxygen present was in multiphase intergranular and intragranular inclusions. The inclusions consisted mainly of turbostratic graphite fibrous crystals dispersed in a silicon oxycarbide glass matrix. The presence and appearance of these inclusions was remarkably consistent (Braue et al., 1994; Das Chowdhury et al., 1993b). The graphite crystals formed by exsolution from the silicon oxycarbide glass during cooling. HRTEM showed that the graphite crystals formed with only one orientation in intragranular inclusions, but formed in many orientations in intergranular inclusions (at triple junctions), indicating that the graphite nucleated heterogeneously from the cooling glass onto SiC grain surfaces. We have also observed these inclusions in Al_2O_3 matrix/SiC whisker composites densified without sintering aids (Braue et al., 1990).

These inclusions are the "other" typical oxygen-containing microstructural defect in ceramics, in addition to the ubiquitous thin amorphous phases often observed at grain boundaries or heterophase interfaces. We have typically observed the inclusions in ceramics densified *without* the addition of *oxide* densification aids during processing.

2. Metal/6H-SiC silicon-terminated (0001) Interfaces

Interfaces between metals and SiC are the basis for important metal matrix composites and contacts for high temperature SiC-based solid state electronic devices. We have investigated ultra-pure interfaces between Ti, Hf, Ti-Hf alloys, Pt, and Co and Si-terminated (0001) 6H SiC single

crystals for the first time. The interfaces were synthesized under UHV high purity conditions by evaporative deposition. This method eliminated the uncertainties induced into earlier investigations of these interfaces by variable substrate orientation and poorly controlled impurity chemistry. This is a collaborative project with Prof. Bob Davis' group at N.C. State University. The interfaces were synthesized using MBE equipment there, on single crystal substrates from Cree research, and analyzed here at ASU.

2.1. Ti/SiC Interfaces (Bow et al., 1993; Porter et al., 1995a).

Ti films 4 to 1000 Å thick deposited at room temperature were epitaxial single crystals. The basal planes and close-packed directions were coincident in both phases. The SiC wafers used for all metal film studies on this project were vicinal, with surface normal tilted 3-4° away from (0001) toward (11 $\bar{2}$ 0). The calculated misfit strain in the interface was about 4%, with Ti in tension and SiC in compression. The defects observed in these interfaces were lattice distortions in both phases at steps on the wafer surfaces and stand-off misfit dislocations in the softer lower-modulus Ti phase about 10Å from the interfaces. Lattice distortions at the steps extended about 17Å into the Ti (seven (0002) planes) and about 8Å into the SiC. The structural width of the interface, determined quantitatively from digitized HRTEM images of defect-free regions was 2.4Å. No impurities or solute gradients were detected in these interfaces by high spatial resolution position resolved EELS or EDS nanospectroscopy, so the chemical width was equal to the structural width.

After post-deposition annealing for 20 to 60 min at 700°C in UHV interface reaction had occurred. The products were hexagonal Ti₅Si₃ and cubic TiC. The silicide formed a nearly continuous polycrystalline layer between the SiC and Ti, with TiC at the SiC/silicide and silicide/Ti interfaces. The reaction zone thickness was about 13nm for this reaction time range. All interfaces remained flat, characteristic of solid state reactions. Nanospectroscopy results showed that about 15 at.% carbon was in solution in the silicide and that the carbide was not stoichiometric. Large solute gradients (i.e. chemical widths) were observed at all interfaces. The misfit strains have been calculated and measured. A thermo-kinetic interface reaction model showed that TiC is the expected first reaction product, but that Ti₅Si₃, which is more stable, will dominate the reaction zone after sufficient reaction time. Computer modeling was used to generate unrelaxed structural models of the Ti₅Si₃/TiC/SiC interfaces in this complex materials system (Bow, 1994a).

2.2. Hf and Ti-Hf alloy films on 6H-(0001) SiC (Bow et al., 1993; Bow, 1994a; Bow, 1994b).

As deposited Hf thin films exhibited three layers of contrast parallel to the SiC substrate in HRTEM images, in the usual edge on orientation. The first two were nanocrystalline and had thicknesses extending ~ 80 and 240 Å, respectively. The third layer contained columnar grains separated by relatively low angle boundaries. This layer was 130 Å thick and extended to the film free surface. The calculated basal plane epitaxial misfit strain magnitude between 6H-SiC and Hf is nearly the same as for Ti, but the sense is reversed. Hf would be in compression and SiC in tension if epitaxy were maintained, but that was not observed. These films contained a very high defect density compared to Ti/SiC.

Post-deposition UHV annealing of the Hf films for 20min @ 700°C produced an easily visible reduction in defect density. The reduction resulted from oriented grain growth in the Hf films. Nanodiffraction showed that close packed directions in the coincident basal planes of both the SiC and the Hf were nearly aligned after the anneal, but the Hf film was still polycrystalline. After 60min UHV annealing @ 700°C a thin reaction zone ~ 15nm wide, in which crystallinity was disturbed, had formed at the Hf/SiC interface. Nanospectroscopy showed that very limited Hf diffusion into SiC had occurred. No Si or C diffusion into Hf was detectable. This zone is evidently the first stage of interfacial reaction between Hf and SiC. The reaction in this case was less advanced than the Ti/SiC reaction after the same time-temperature cycle, presumably because Hf, whose melting point is ~550°C greater than the Ti melting point, is less mobile and reactive toward SiC.

The difference in unit cell lattice constants between Ti and Hf indicated that a Ti-Hf alloy of approximately equiatomic composition should have perfect basal plane lattice matching with 6H-SiC, leading to an excellent rectifying contact. We examined such an alloy film, made by UHV co-deposition, in the as-deposited condition. The film structure was a single crystal epilayer, however perfect lattice matching was not obtained. Standoff misfit dislocations were observed in the alloy film, but with wider spacing than in the Ti epilayer described above, indicating a better lattice match had been achieved. Applications of new chemically sensitive hollow cone and energy-selected spectroscopic transmission electron imaging to the alloy film showed that it was chemically heterogeneous, i.e. the lattice constant varied along the interface. The average lattice constant was larger than Ti, but the match with the SiC substrate was not as good as it would have been for a chemically homogeneous film. The chemical heterogeneity observed using the new chemically sensitive imaging methods was verified by conventional position-resolved x-ray nanospectroscopy. The heterogeneity resulted from instabilities in the co-evaporation film deposition process.

2.3. Pt and Co films on 6H-SiC (0001) substrates (Bow et al., 1993; Porter et al., 1995b; Porter et al., 1995c).

Both Pt and Co are used to form rectifying contacts on Si, so these metals are potential contact materials for SiC, as well as being useful model examples of metal/SiC composite interfaces. The thermal stability of these interfaces, particularly under high purity conditions, was relatively unknown, and we have reported initial results. Note carefully that both of these metals form stable silicides just as Ti and Hf do, but they do not form highly stable carbides whereas Ti and Hf do so. The major differences observed between Pt and Co interface reaction morphology and the Ti and Hf interface reactions seem to be related to this difference in carbide stability. The deposition procedure used for Pt and Co was the same as for the metals above.

The as-deposited Pt films were 8 to 15 nm columnar-grained polycrystals. There was no well-defined epi relationship with the substrate. After annealing at 550°C for 20 min preferential oriented grain growth had occurred. The remaining grains were at least 40 nm in size, and had a well defined $\{111\} // (0001)$, $\langle 220 \rangle // \langle 11\bar{2}0 \rangle$ crystallographic habit with the SiC substrate. The interface was atomically flat except for small vicinally-induced steps. Only the presence of twins in some of the Pt grains indicated the presence of growth induced strains or defects. No interdiffusion was detectable by nanospectroscopy, and there was no other indication of interface reaction. Unrelaxed atomic crystal modeling showed that atom matching across the interface with this orientation was quite good. However, conventional misfit strain calculations based on lattice constants indicated that this orientation was highly strained, and that the calculated strains could be significantly reduced if the Pt crystals were rotated 30° about the interface normal. The absence of the latter habit relation indicated that atom matching across the film/substrate interface dominated the habit self-selection.

After 20min @ 650°C post-deposition annealing the Pt/SiC interface reaction had just initiated, by formation of a few isolated reaction zones along the interfaces where Pt had penetrated *into* the SiC, up to ~10nm. The bottom of the reaction zones and the unreacted interface remained flat and parallel to (0001) SiC, but the edges of the zones were atomically rough and essentially perpendicular to the SiC basal planes. The reaction product was a metastable Pt(Si, C) solution. In addition, a few small amorphous regions were seen at the position of the original Pt/SiC interface. After 20min @ 750°C post-deposition annealing, extensive reaction zones had formed by penetration of Pt into the SiC to depths of 45 to 60 nm. The bottoms of the zones were flat and parallel to (0001) SiC. Changes in reaction zone depth occurred at steps several nm high nearly perpendicular to the reaction zone/substrate interface. This geometry indicates the zones formed heterogeneously by penetration into the SiC, as first observed after 650°C annealing. The zones widened apparently by lateral motion of the bounding steps during subsequent interface reaction. Observations of the reaction zones formed at 750°C showed that the lateral zone widths were much larger than the heights of the nearly vertical steps separating zone regions of differing penetration depth into the SiC substrate, indicating that the zone-formation reaction rate was larger parallel to

the SiC {0001} planes of the substrate than it was perpendicular to them, in the direction of increasing depth. The internal zone microstructure consisted of a thin discontinuous layer of Pt₂Si adjacent to the substrate, and a thicker multiphase layer, containing amorphous and crystalline carbon, Pt(Si, C) solution, small Pt₂Si particles and voids, extending upward to the unreacted Pt. The phase boundaries in this region were smoothly curved, suggesting that interface melting occurred during reaction zone formation, and that these product phases formed by exsolution and precipitation from the liquid. Nanospectroscopy showed that wide chemical widths existed at phase boundaries in the zones after the 750°C annealing. Chou (1991a, 1991b) made similar lower resolution observations of reaction zone morphology during his investigation of Pt/ β -SiC diffusion couples and stated that interface melting had occurred at 900°C, 1000°C, and 1100°C.

Co deposited on the vicinal SiC substrate in the hexagonal form, as a columnar grained polycrystalline film. Strong epitaxy was not observed. Co grain basal plane normals were within $\pm 5^\circ$ of the substrate [0001] normal for some grains, but there was rotational disorder in the basal planes. HRTEM images showed large strain contrast in the film, and the Co was twinned. This interface is a large misfit material system. If the epi relation observed for Ti/SiC were present here, the misfit could be as large as 18%. We also observed an ~ 0.34 nm thick layer of low contrast and high disorder that was nearly continuous along the interface, which did *not* correspond to impurity segregation according to our nanospectroscopy results. This type of contrast has been observed in other large misfit heterophase metal/ceramic and ceramic interfaces by HRTEM (Merkle et al., 1992; Xiao et al., 1992), and attributed to delocalized large misfit strains. Merkle et al. noted that chemical segregation could be important for this effect, but that little data was available. Our results on narrow (~ 0.3 nm) Si₃N₄ disordered grain boundaries showed that *both* HRTEM and nanospectroscopy are required to establish the presence of segregation. This nearly continuously disordered Co/SiC interface may be the first example of such an interface without segregation in a metal/ceramic system (Bow, 1994a). This interface exhibited excellent rectifying behavior.

We examined these Co/SiC interfaces after 2min @ 1000°C rapid thermal post-deposition annealing and observed a reaction zone similar to the Pt/SiC case but more advanced, because the reaction temperature was higher. The reaction front had penetrated 100 to 220 nm into the SiC leaving flat steps separated by ledges on the substrate. The multiphase reaction zone contained CoSi, graphite, amorphous carbon, and voids, separated by smoothly curved interfaces indicating that interface melting had occurred, in qualitative agreement with other *ex situ* results (Chou et al., 1991b). We observed wide chemical widths at reaction zone interfaces and detected Si diffusion into all parts of the Co film. Interestingly, the graphitic and amorphous carbon reaction zone morphologies in Co/SiC and Pt/SiC have a strong resemblance to the graphite fiber amorphous matrix inclusions we observed in ceramic systems, noted above (Braue et al., 1994; Das Chowdhury et al., 1993b; Braue et al., 1990), except of course, the matrices in the metal/SiC systems are not silicon oxycarbide glass. The observations imply that the formation mechanisms may be similar, exsolution of some form of carbon from a supersaturated solution upon cooling, in the absence of carbide compound formation. Co/SiC formed an ohmic contact after interface reaction.

The electronic behavior of metal/SiC contacts has been recently reviewed (Porter and Davis, 1995). The metal/SiC couples studied have usually been extensions from metal/Si research. Metal/Si contacts usually yield Si-rich silicide reaction products, while metal/SiC contacts are expected to yield metal-rich silicide products and usually did, provided the metal film is not completely consumed. Most metals form rectifying contacts on p- and n-type SiC with ~ 1 eV Schottky barrier height (SBH). The SBH of as-deposited contacts usually increases a few tenths of an eV upon annealing, which has been attributed qualitatively to an increase in "perfection" of the interface by many authors. Few high resolution studies of these interfaces have been done. Ohmic contacts are much harder to make. Only annealed Co/SiC was ohmic in the present work. The present results showed that interface microstructure in most cases is complex, particularly after reaction, and quantitative relations between microstructure, rectifying or ohmic behavior and SBH magnitude is an open field for future research. It is apparent from the literature that chemical impurity control differs widely among research groups working on interfaces of all kinds. Our

materials are among those most closely controlled. We believe such control is critical, especially to understand effects such as interface melting.

3. Methods and Instrumentation

3.1. Imaging the chemistry and structure of interfaces/boundaries.

Conventional phase contrast HRTEM imaging at 0.18nm resolution (Topcon 002B 200KV microscope) was used for imaging structure in the present work. Chemical widths and nanospectroscopy were done using a field emission Philips 400 microscope fitted with a computer control system designed and built here that provides position-resolved and time-resolved nanospectroscopy capability (Weiss et al., 1992). We have experimentally and theoretically determined the focused probe current distribution as a function of electron optical parameters for this microscope, thus probe size is known quantitatively (Weiss et al., 1991). These were the primary methods used for the interface/boundary research above.

We evaluated direct and indirect chemically sensitive imaging methods for detection of segregation.

We used our Zeiss 912 Ω TEM for energy selected imaging of sintering aid distributions at grain boundaries in the Si₃N₄/SiC(w) composites (Carpenter et al., 1995a). This analytical imaging method is spectroscopic, based on EELS; the physics were recently described in detail (Reimer, 1995). This is a parallel method that produces a real space image with high contrast in the specimen regions having a high content of the element whose absorption edge is selected for imaging. The method works well for fast low magnification survey of elemental distributions: oxygen and aluminum images exhibited high contrast at grain boundaries and triple junctions and silicon and nitrogen images conversely exhibited low contrast in the same specimen regions, in excellent qualitative agreement with our nanospectroscopy results. However the detection sensitivity (minimum detectable mass fraction (MDMF), Isaacson and Johnson, 1975) is smaller than for small FEG probe nanospectroscopy, because the incident current density of the defocused thermionic-source illumination imaging beam is much smaller than for a focused FEG probe, viz. 5 compared to 10⁵ amps/cm². MDMF is proportional to (Jt)^{-1/2}, where J is incident flux and t is image collection time. This poorer detection sensitivity causes the long tails of the chemical widths to be "cut off", i.e. lost in statistical background noise, so that the chemical widths appear much smaller than the widths observed using FEG nanospectroscopy methods, although still larger than the corresponding structural widths. Specimen drift precluded extending image collection times to large values sufficient to overcome this MDMF problem. Thus, energy-selected imaging is a fast convenient method for *surveying elemental distributions present at relatively high concentrations over large specimen areas*, or for *phase identification*, and it will be used for that purpose.

Z-contrast STEM imaging and its TEM analog, hollow cone imaging, were used to detect yttrium chemical widths at grain boundaries and interfaces in the Si₃N₄/SiC(w) composites and to detect inhomogeneous Hf distributions in evaporated Ti-Hf films with excellent results (Bow, 1994b; Das Chowdhury, 1995; Liu et al., 1993). Contrast, i.e. intensity, in these images depends on local atomic number, Z, for specimens of constant thickness (Dinges et al., 1994; Jesson and Pennycook, 1993, 1995; Liu and Cowley, 1993). These are indirect and not spectroscopic methods. We verified our Z-contrast results using nanospectroscopy. These methods produced results in excellent qualitative agreement with nanospectroscopy, and in closer quantitative agreement than energy-selected imaging. In addition, these methods have high resolution potential equal to conventional HRTEM, and will be pursued further.

3.2. Interface and boundary synthesis.

The effect of chemical impurities on interface/boundary structure and properties is one of the primary interests of this research. Of the many types of interfaces and boundaries we have examined to date, all except those made by special high purity CVD or MBE methods contained impurity distributions of varying and uncontrollable magnitude. In addition, most of the interfaces

had complex shapes that were difficult for most types of structure or properties analysis. We have designed and constructed an *interface synthesis unit*, to make planar interfaces under conditions of very high purity and also with closely controlled impurity conditions, to analyze the effects of impurities on structure and properties. The interfaces are made by preparing two substrates simultaneously, which form the two sides of the interface, and then inverting one onto the other and bonding to form the interface. Insitu substrate preparation includes cleaning the surfaces by Xe or Ar ion bombardment and/or heating, followed by controlled impurity deposition if desired. The vacuum system environment of the synthesis unit is not opened during the several step cleaning, deposition, bonding process.

Equipment for the unit was purchased on DOE University Instrumentation Grant DE-FG05-93ER79234. Design and construction has been supported by the present grant. Design is now complete and construction is nearly finished. The unit design is shown in Fig. 1.

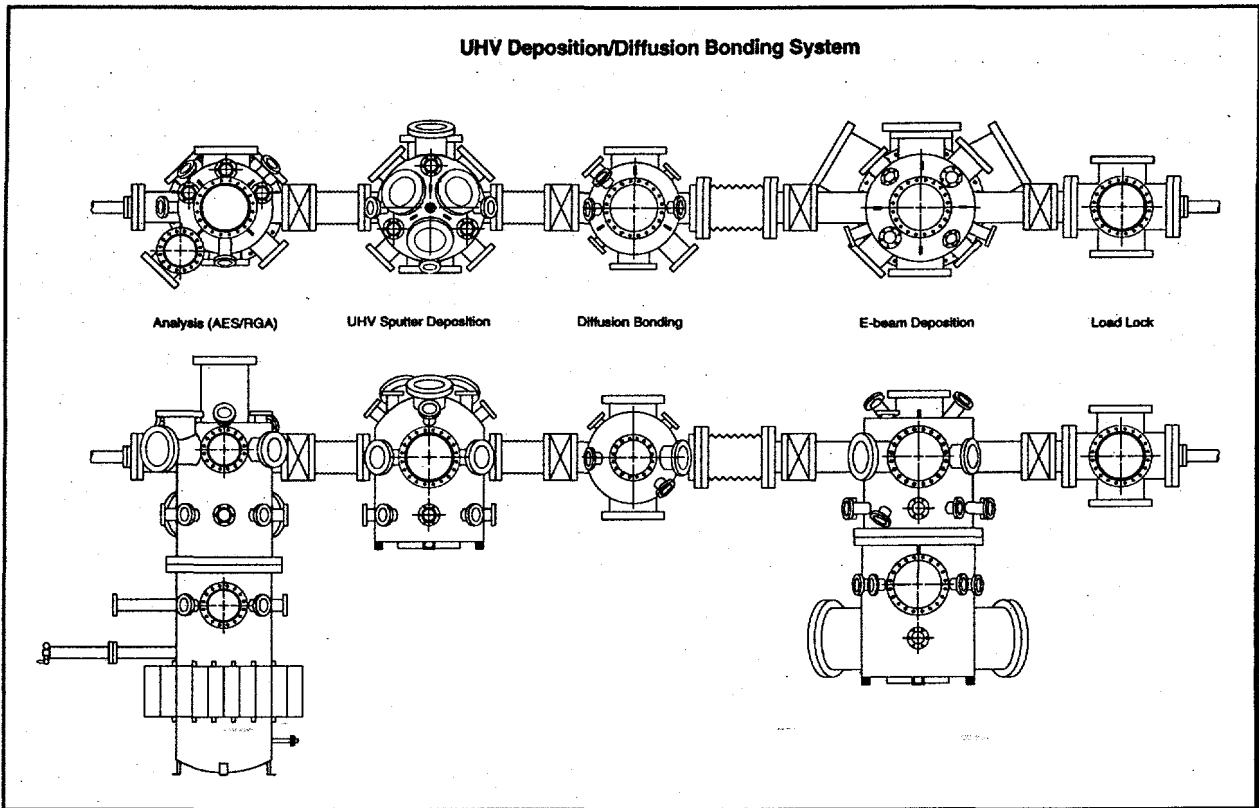


Fig. 1. Schematic view of UHV Deposition/Diffusion Bonding Unit for interface synthesis.

The load lock, deposition/RHEED and diffusion bonding chambers are all assembled and tested, and have already been used to synthesize specimens. The base pressure attained in the deposition/RHEED and diffusion bonding chambers is mid 10^{-10} torr. The deposition chamber contains eight stations (crucibles) for e-beam deposition on planar substrates prior to bonding without breaking vacuum, presently loaded with Ta, Nb, Ti, Si, Ag, Al, and Cu. We have successfully deposited the highest melting of these, Ta, without equipment overheating or power shortage problems. Bonding chamber performance is excellent. It will maintain a pressure of 10^{-9} torr with the specimen in the 400 to 500°C range, and low 10^{-8} torr with Al_2O_3 specimens at 950°C, using 75% power without chamber overheating. We expect to be able to reach close to 1200°C specimen temperature during bonding when necessary. The compressive load on the interface specimen assembly is applied by a computer controlled load frame containing a load cell (2000 lbs. maximum load). The feedback control loop permits maintenance of constant load during temperature changes, or a programmed variable load cycle.

The system as it appears now is shown in fig. 2.

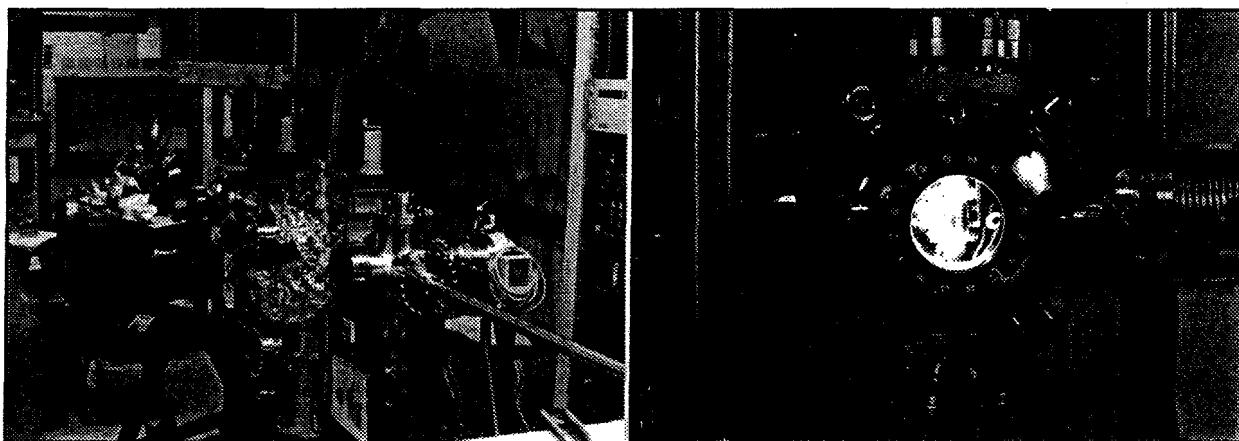


Fig 2. UHV Deposition/Diffusion Bonding Unit. The left image shows the load lock, deposition, and diffusion bonding chamber viewed from near the the right end. The right image shows the bonding chamber with an Al_2O_3 specimen in it at 950°C .

The left image shows the load lock, deposition/RHEED, and bonding chambers, foreshortened by viewing at a small angle from the right. The length of the unit is about fifteen feet. The load frame is visible around the bonding chamber at center, and the Auger unit, not yet connected to the main unit, is visible in the background. The right image shows the hot zone through the front port, containing an Al_2O_3 interface specimen at 950°C .

The reactive UHV sputter chamber is built to our design, and will be delivered at the end of summer. It includes gas dosers located at the substrate specimen surfaces and substrate heating/temperature control. It will provide capability for sputter deposits from compound or metal targets onto one or both substrates, which can be reacted with gas from the dosers if necessary to form particular interface layers, prior to bonding. This chamber, together with the deposition/RHEED chamber, will provide good control over impurity distributions in planar interfaces whose structure and properties we will study.

The scanning Auger spectrometer, which we will use for substrate composition examination prior to bonding, requires a new UHV upper specimen chamber to mate properly with the rest of the unit. It is being built to our design and will be delivered at the end of summer with the sputter chamber.

We have synthesized planar interfaces of both polycrystalline and single crystal (sapphire) Al_2O_3 with thin interface layers of copper and stainless steel with and without thin interface layers of titanium very successfully to date.

3.3. Energy selecting environmental cell HRTEM microscopic materials research.

Interface reaction mechanisms and kinetics are important. Recent results show that they can change the mechanical behavior of composite interfaces (Braue and Kleebe, 1996) and the electronic behavior of contacts on SiC (Porter et al., 1995a, 1995b, 1995c). These results and our current results on interface reactions at interfaces in TiN/GaN/AlN/SiC multilayers (Huang et al., 1995; Liu et al., 1996) show that the reactions are nucleated heterogeneously, presumably at one or more of the several types of defects observed at the interfaces. Identifying the important defects in these cases is somewhat more difficult than in the case of many heterogeneously nucleated bulk reactions, e.g. precipitate nucleation on a dislocation line. Similar comments apply to interface reactions in which local melting is thought to be important.

We are assembling an HRTEM/environmental cell/Gatan energy filter microscope to study selected interface reaction mechanisms insitu in controlled reactive or inert gaseous environments at elevated temperature. Our Philips EM 430 HRTEM, with point resolution of $\sim 2\text{\AA}$ at 300kV, and

slightly less at 200kV, is being used for this project. The environmental cell is of our own design. The prototype has been built and successfully tested on our Philips EM 400. The Gatan imaging energy filter (GIF) is functionally similar to the Ω filter on our Zeiss 912 Ω TEM, but it is mounted after the final projector lens at the end of the electron optical path on the EM 430, instead of adjacent to the objective lens, so it does not interfere with installation of the environmental cell. The optics of the GIF are well understood (Krivanek et al., 1991). The GIF functions as an energy-selected spectroscopic imaging device or conventional EELS spectrometer (Carpenter et al., 1995a) and it does not limit the electron optical resolution of the microscope (Hashimoto et al., 1992). The GIF can also operate as a filter, to reduce chromatic aberration blurring in thick specimen images. This is an important advantage for insitu microscopy, because it is often necessary to compare reactions in thick and thin areas, to be sure that free surface effects are not obscuring the mechanism. All of the hardware necessary for this project has been ordered and received. Construction and assembly has begun. It will be completed and ready for materials research use in the spring of 1997. The project equipment acquisition is supported by USDOE University Research Instrumentation Grant DE-FG03-95TE00068. Dr. Renu Sharma, Research Scientist and faculty member in the Science and Engineering of Materials Program, and Mr. Karl Weiss, Research Specialist, of the Center for Solid State Science are major participants in this project.

This microscope system will be used for the proposed research, in mid-1997.

4. Theory

4.1. HRTEM imaging.

We achieved major progress in understanding the anomalous subunitcell contrast observed in 6H-SiC high resolution images by several investigators, and most recently by us during our work on metal/6H-SiC interfaces. At the same time we also observed similar anomalous contrast in HRTEM images from other hexagonal crystals, e.g. Ti and Ti₅Si₃. Such contrast for 6H-SiC has been variously attributed, e.g. to crystal misalignment, incident beam tilt, and chemical ordering or segregation in the SiC. Since our work dealt with diffusion controlled interface reactions on 6H-SiC, there was a very real possibility that this contrast could be related to the reactions, and a quantitative explanation became necessary. We did extensive theoretical image computations as functions of crystal tilt and thickness, using the same electron optical parameters we used for experimental imaging, first for 6H-SiC, and then for other hexagonal materials whose images exhibited the anomalous contrast. The results showed that the anomalous contrast resulted from anisotropic smearing of the crystal scattering potential *inside the unit cell* when the crystal was tilted slightly off the imaging zone axis. The strength of the anomalous contrast depends on both the tilt angle magnitude and its azimuth. Tilted, real-space computed crystal models provided the first physical visualization and understanding of this effect (Bow et al., 1996). The anomalous contrast strength increases with crystal thickness, but it will not occur for any specimen thickness when the crystal is oriented exactly on the imaging zone axis. From the diffraction viewpoint, the effect occurs because small crystal tilts cause violations of Cowley-Moodie dynamical extinction rules, i.e. for tilted crystals the incident electron beam direction lies *outside* the black zero order Gjonnes-Moodie extinction lines. These bands result from the existence of certain translational symmetry elements in the space groups of hexagonal crystals, i.e. screw axes and glide planes. Our results showed that this anomalous contrast does not occur in HRTEM images for similarly tilted crystals that do not contain these symmetry elements, e.g. β -SiC and TiC, both of which are cubic. Very small tilting errors will cause the anomalous contrast in hexagonal crystal HRTEM images, only fractions of a degree. Such small errors are essentially impossible for an experimentalist to avoid, so this anomalous contrast will be observed often, but it is not an indicator of short or long range chemical order, even in systems where reactions have occurred. By analogy, similar anomalous HRTEM contrast should occur in images with small tilting errors, for any crystals that contain symmetry elements that will induce dynamical extinctions, but there is not much comment on this topic in the literature.

Crystalline interfaces such as those resulting from metal/6H SiC reactions often have multiple layers, for example the $\text{Ti}_5\text{Si}_3/\text{TiC}/6\text{H-SiC}$ triad. In this case the TiC interlayer was only $\sim 25 \text{ \AA}$ thick normal to the plane of the interfaces. For structural interface analysis it is necessary to simulate both interfaces in the multilayer, because as the TiC midlayer becomes thinner the two interfaces will begin to affect each other's structure. We have developed a method for this (Bow et al., 1994) using sequential construction of two supercells in which the crystal models are assembled with suitable translation vectors. Blocks of 6H-SiC and TiC with crystal faces and relative crystallographic orientation matching the experimental observations were assembled with relative translation vector placing the Ti atoms for a Ti-terminated carbide crystal at the centers of tetrahedra formed by Si atoms on the Si-terminated (0001) SiC surface. This supercell was then matched with a Ti_5Si_3 crystal having the observed crystallographic relationship and facets, and one of several possible translation vectors which determine atom matching across the interface. The total supercell was $62 \times 20 \times 20 \text{ \AA}^3$ in size, and contained 805 carbon atoms, 660 silicon atoms, and 644 titanium atoms. Simulation computations required about 20 min. CPU time on a Silicon Graphics Personal Iris 4D/35 work station, thus the computations are feasible. The total supercell can easily be tilted, and images for small tilts off the exact imaging zone axis exhibited the anomalous subunitcell contrast noted above in the hexagonal regions of the supercell, just as the experimental images did. Other specimen variables that can be controlled for the simulation computations are thickness, faceting, relative crystallographic orientation, and translation vectors of the three phases. We can also include relaxation at the interfaces and more than three phases, with some increase in computation time. The results so far are good and justify further development of the method.

5. Students graduated, and Students and Postdocs with research supported by this project

J.S. Bow completed his Ph.D. work on this project and graduated in the summer of 1994. He won a Microscopy Society of America Distinguished Presidential Scholarship in August of 1994 for his original application of TEM Hollow-cone imaging, HRTEM, and energy-selected imaging to analysis of Ti and Hf distribution in thin Ti-Hf alloy thin films deposited on single crystal 6H-SiC. He is now employed as group leader for Microstructural Analysis and Surface Analysis at the Industrial Technology Research Institute in Taiwan. His Institute has many materials collaborations with US laboratories and he visits the U.S. often.

K. DasChowdhury stayed on this project as a Postdoc until 1994. Then he successfully completed a post-doctoral appointment at MIT, in early 1995, and joined Intel Corporation as a Senior Analytical Engineer at their new fabrication facility in Rio Rancho, N.M. near Albuquerque. In the early summer of 1996 Intel gave him their corporate Pentium Divisional Recognition Award, their second highest corporate award, for pioneering application of TEM/STEM analysis to discover Sodium contamination in dielectric layers of electronic devices.

Current students receiving doctoral research support from this project are:

1. Jin Xu, B.S. in Materials Science and Engineering. She is working on the interface synthesis unit. Expected graduation in 1997.
2. Michael Cox, B.S. in Materials Science and Engineering. He is currently working on the interface synthesis unit. Expected graduation in 1998.
3. Rou-Jane Liu, B.S., M.S. in Physics. She is working on high resolution analysis of interfaces. Expected graduation in 1998.
4. Jiawen Jin, B.S. in Materials Science and Engineering. He is working on high resolution analysis of interfaces. Expected graduation in 2000.

Both Dr. DasChowdhury and Dr. Bow completed their doctorates in the Science and Engineering of Materials (SEM) Program. All of the students are also enrolled in this highly regarded interdisciplinary Program. The SEM Program emphasizes the solid state science aspects of Materials Science and Engineering, and has produced 21 successful graduates since 1991. A complete description of the Program is given on its Web page, whose URL address is <http://www.asu.edu/graduate/SEM/>.

Important collaborators with us on this project are:

Dr. Wolfgang Braue, German Aerospace Research Establishment, Cologne, Germany, for ceramics research.

Prof. Robert F. Davis, Department of Materials Science and Engineering, North Carolina State University, for metal/SiC and SiC/AlN/GaN/Metal interfaces research.

Dr. M. J. Kim, Research Scientist, Center for Solid State Science, Arizona State University, for HRTEM and interface synthesis. He is an SEM faculty member.

Dr. Renu Sharma, Research Scientist, Center for Solid State Science, Arizona State University, for HRTEM/environmental cell/energy-selected imaging materials research. She is SEM Program faculty member.

Prof. Karl Sieradzki, Department of Mechanical and Aerospace Engineering, Arizona State University, for mechanical properties. He is a member of the SEM Program faculty.

6. Publications from project for last three years

"Local Chemistry at Interfaces and Boundaries: Ceramic and Electronic Composite Materials," R.W. Carpenter, J.S. Bow, M.J. Kim, K. Das Chowdhury and W. Braue, invited keynote paper at the Carmelo DiBlasi Symposium, University of Lecce, Italy, Microscopy, Microanalysis, Microstructures 6, 587-599 (1995).

"Crystallographic Origin of the Alternate Bright/Dark Contrast in 6H-SiC and Other Hexagonal Crystal HREM Images," J.S. Bow, R.W. Carpenter and M.J. Kim, J. Micros. Soc. Amer. 2, 63-78 (1996).

"Chemistry, Microstructure and Electrical Properties at Interface Between Thin Films of Titanium and Alpha (6H) Silicon Carbide (0001)," L.M. Porter, R.F. Davis, J.S. Bow, M.J. Kim and R.W. Carpenter, J. Mater. Res. 10(3), 668-678 (1995).

"High Resolution TEM and AEM Study in (Au, TiN) Thin Film on (100) Silicon," J.S. Bow, Y.C. Hung, M.J. Kim, R.W. Carpenter, W.M. Kim, S.K. Lee and S.G. Kim, Proc. 53rd Ann. Mtg. Micros. Soc. Amer., 554-555 (1995).

"An HREM Study of the Microstructure of Al Contact on GaN/AlN/SiC Thin Films," Y. Huang, L. Smith, M.J. Kim, R.W. Carpenter and R.F. Davis, Mater. Res. Soc. Symp. 355, 433-439 (1995).

"Chemical Widths at Composite Interfaces: Relationships to Structural Widths and Methods for Measurement," R.W. Carpenter, J.S. Bow, M.J. Kim, K. DasChowdhury and W. Braue, Mater. Res. Soc. Symp. 357, 221-277 (1995).

"Chemical and Structural Widths of Interfaces and Grain Boundaries in Silicon Nitride-Silicon Carbide Whisker Composites," K. DasChowdhury, R.W. Carpenter, W. Braue, J. Liu and H. Ma, J. Amer. Ceram. Soc. 78, 2579-2592 (1995).

"Chemical and Structural Width of Interfaces and Grain Boundaries in Ceramic Composites," R. W. Carpenter, K. DasChowdhury, W. Braue and J. Liu, Proc. 13th Inter. Conf. Elec. Micros. (ICEM-13) 2A, 257-258 (1994).

"HREM Image Simulation of Ti₅Si₃/TiC/6H-SiC Interfaces," J.S. Bow, R.W. Carpenter and M.J. Kim, Proc. 52nd Ann. Mtg. Micros. Soc. Amer., Ed. by G.W. Bailey and A.J. Garratt-Reed, San Francisco Press, 518-519 (1994).

"Analysis of Co-deposited Ti-Hf Thin Film on (0001) 6H-SiC by HREM, Energy-Selected and Hollow-Cone Images," J.S. Bow, Proc. 52nd Ann. Mtg. Micros. Soc. Amer., Ed. by G.W. Bailey and A.J. Garratt-Reed, San Francisco Press, 978-979 (1994).

"Oxygen Sinks in SiC-Based Ceramics," W. Braue, K. DasChowdhury and R.W. Carpenter, Proc. Symp. Covalent Ceramics II: Non-Oxides, Mater. Res. Soc. Symp. 327, 275-280 (1994).

"Deposition and Characterization of Schottky and Ohmic Contacts on n-type alpha (6H)-SiC (0001)," L.M. Porter, R.F. Davis, J.S. Bow, M.J. Kim and R.W. Carpenter, Proc. 5th

- Inter. Conf. Silicon Carbide and Related Materials, Washington D.C., 1993, Inst. Phys. Conf. Ser. 137, 581-584 (1994).
- "HREM and AEM Study of Pt/SiC Interface Annealed at High Temperature," J.S. Bow, L.M. Porter, M.J. Kim, R.W. Carpenter and R.F. Davis, Proc. 51st Annual EMSA Meeting, Cincinnati, OH 1993, Ed. G.W. Bailey and C.L. Rieder (San Francisco Press, San Francisco, CA, 1993) 832-833 (1993).
- "Preparation of Thin-Film Metal/6H-SiC TEM Specimens by RPR Ion Milling," J.S. Bow, F. Shaapur, M.J. Kim and R.W. Carpenter, Proc. 51st Annual EMSA Meeting, Cincinnati, OH 1993, Ed. G.W. Bailey and C.L. Rieder (San Francisco Press, San Francisco, CA, 1993) 714-715 (1993).
- "Grain Boundaries in Silicon Nitride," K. DasChowdhury, R.W. Carpenter and W. Braue, Proc. 51st Annual EMSA Meeting, Cincinnati, OH 1993, Ed. G.W. Bailey and C.L. Rieder (San Francisco Press, San Francisco, CA, 1993) 920-921 (1993).
- "Origin of the Alternate Bright/Dark Contrast in HREM Images of Hexagonal Crystals, Particularly 6H-SiC," J.S. Bow, R.W. Carpenter and M.J. Kim, Proc. 51st Annual EMSA Meeting, Cincinnati, OH 1993, Ed. G.W. Bailey and C.L. Rieder (San Francisco Press, San Francisco, CA, 1993) 914-915 (1993).
- "Thin Film Ti/6H-SiC interfacial reaction: High Resolution Electron Microscopy Study," J.S. Bow, L.M. Porter, M.J. Kim, R.W. Carpenter and R.F. Davis, Ultramicroscopy 52, 289-296 (1993).
- "Chemical and Electrical Mechanisms in Titanium, Platinum, and Hafnium Contacts to Alpha (6H) Silicon Carbide," L.M. Spellman, R.C. Glass, J.S. Bow, M.J. Kim, R.W. Carpenter and R.F. Davis, Mater. Res. Soc. Symp. 282, 471-477 (1993).
- "High Spatial Resolution TEM Study of Thin Film Metal/6H-SiC Interfaces," J.S. Bow, L.M. Spellman, M.J. Kim, R.W. Carpenter and R.F. Davis, Mater. Res. Soc. Symp. 280, 571-576 (1993).
- "Elemental Analysis of Matrix Grain Boundaries in SiC Whisker Reinforced Si₃N₄ Based Composites," J. Liu, K. DasChowdhury, R.W. Carpenter and W. Braue, Mater. Res. Soc. Symp. 287, 329-334 (1993).
- "A Microstructural Study of Reaction-Bonded Silicon Carbide," K. DasChowdhury, R.W. Carpenter and W. Braue, Mater. Res. Soc. Symp. 295, 183-188 (1993).
- "Ab Initio Calculation of Band Structure, X-ray Emission, Quantum Yield and Electron Energy Loss Spectra of Hexagonal Boron Nitride," H. Ma, S.H. Lin and R.W. Carpenter, P. Rice and O.F. Sankey, J. Appl. Phys. 73, 7422-7427 (1993).

7. References

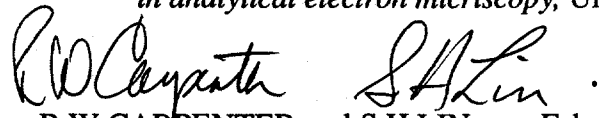
- J.S. Bow, R.W. Carpenter, and M.J. Kim (1996), *Crystallographic Origin of Alternate Bright/Dark Contrast in 6H-SiC and other Hexagonal Crystal HREM Images*, Jour. Micros. Soc. Amer. 2(2), 63-78.
- J.S. Bow, R.W. Carpenter, and M.J. Kim (1994), *HREM Image Simulation of Ti₅Si₃/TiC/6H-SiC Interfaces*, Proc. 52nd Ann. Mtg. Micros. Soc. Amer., San Francisco Press, Inc., San Francisco, 518-519.
- J. S. Bow (1994a), *HREM and AEM Study in Metal/6H-Silicon Carbide Interfaces Synthesized by Ultra High Vacuum/Molecular Beam Epitaxy*, Doctoral Dissertation, Science and Engineering of Materials Program, Arizona State University.
- J. S. Bow (1994b), *Analysis of Co-Deposited Ti-Hf Thin Film on (0001)6H-SiC by HREM, Energy-Selected, and Hollow-Cone Images*, Proc. 52nd Ann. Mtg. Micros. Soc. Amer., ed. by G.W. Bailey et al., San Francisco Press, 978.
- J. S. Bow, L.M. Porter, M.J. Kim, R.W. Carpenter and R.F. Davis (1993), *High Spatial Resolution TEM Study Of Thin Film Metal/6H-SiC Interfaces*, Mat. Res. Soc. Symp. Proc. Vol. 280, 571-576.

- W. Braue, K. Das Chowdhury and R.W. Carpenter (1994), *Oxygen Sinks in SiC-Based Ceramics*, Proc. Symp. Covalent Ceramics II: Non Oxides, ed. A. R. Barron et al., Mater. Res. Soc. Symp. Proc. Vol. 327, 275-280.
- W. Braue, R.W. Carpenter, and D.J. Smith (1990), *High-resolution interface analysis of SiC-whisker-reinforced Si₃N₄ and Al₂O₃ matrix composites*, Jour. Mater. Sci. 25, 2949-2957.
- R.W. Carpenter, J.S. Bow, M.J. Kim, K. Das Chowdhury and W. Braue (1995a), *Chemical Widths at Composite Interfaces: Relationships to Structural Widths and Methods for Measurement*, Proc. Matl. Res. Soc. Symp. Structure and Properties of Interfaces, ed. by D.A. Bonnell, U. Chowdhry and M. Rühle, Mat.Res.Soc.Symp. Vol.357, 271-277.
- R.W. Carpenter, J.S. Bow, M.J. Kim, K. Das Chowdhury and W. Braue (1995b), *Local Chemistry at Interfaces and Boundaries: Ceramic and Electronic Materials*, Microscopy, Microanalysis, Microstructures 6, 587-599.
- R.W. Carpenter, K. Das Chowdhury, W. Braue and J. Liu (1994), *Chemical and Structural Width of Interfaces and Grain Boundaries in Ceramic Composites*, Proc. of the 13th Intern. Conf. on Elec. Micros. (ICEM-13), Vol. 2A, 257.
- K. Das Chowdhury, R.W.Carpenter, W. Braue, J. Liu, and H. Ma (1995), *Chemical and Structural Widths of Interfaces and Grain boundaries in Silicon Nitride- Silicon Carbide Whisker Composites*, J. Amer. Cer. Soc. 78[10], 2579-2592.
- K. Das Chowdhury, R.W. Carpenter, and W. Braue (1993a), *Grain Boundaries in Silicon Nitride*, Proc. 51st Ann. Mtg. Micros. Soc. Amer., ed. by G.W. Bailey and C. Rieder, (San Francisco Press) 920.
- K. Das Chowdhury, R.W. Carpenter and W. Braue (1993b), *A Microstructural Study of Reaction-Bonded Silicon Carbide*, Proc. Symp. Atomic Scale Imaging of Surfaces and Interfaces, ed. D.K. Biegelsen et al., Mater. Res. Soc. Symp. Proc. Vol. 295, 183-188.
- C. Dinges, H. Kohl and H. Rose (1994), *High-resolution imaging of crystalline objects by hollow-cone illumination*, Ultramicros. 55, 91-100.
- R.E. Dunin-Borkowski and W.M.Stobbs (1993), *The Defocus Contrast of a θ' Precipitate in Al-4 wt.% Cu: Fresnel Fringe Analysis Applied to an Atomically Abrupt Interface*, Ultramicros. 52, 404-414.
- H. Hashimoto, Y. Makita, and N. Nagaoka (1992), Optikk 93, 119.
- M. Isaacson and D. Johnson (1975), *The Microanalysis of Light Elements Using Transmitted Energy Loss Electrons*, Ultramicros. 1, 33-52.
- D.E. Jesson and S.J. Pennycook (1993), *Incoherent Imaging of Thin Specimens using Coherently Scattered Electrons*, Proc. Roy. Soc. Lond.A 441, 261-281.
- D.E. Jesson and S.J. Pennycook (1995), *Incoherent imaging of crystals using thermally scattered electrons*, Proc. Roy. Soc.Lond.A 449, 273-293.
- O.L. Krivanek, A.J. Gubbens and N. Delby (1991), Micros. Microanal. Microstruc.2, 315.
- J. Liu and J.M. Cowley (1993), *High-resolution scanning transmission electron microscopy*, Ultramicros. 52, 335-346.
- J. Liu, K. Das Chowdhury, R.W. Carpenter and W. Braue (1993), *Elemental Analysis of Matrix Grain Boundaries in SiC Whisker Reinforced Si₃N₄ Based Composites*, Proc.Symp.Silicon Nitride Ceramics-Scientific and Technological Advances, ed. I.-W. Chan et al., Mater. Res. Soc. Symp. Proc. Vol. 287, 329-334.
- L.M. Porter and R.F. Davis (1995), *A critical review of ohmic and rectifying contacts for silicon carbide*, Materials Science and Engineering B34, 83-105.
- L.M. Porter, R.F. Davis, J.S. Bow, M.J. Kim, R.W. Carpenter and R.C. Glass (1995a), *Chemistry, microstructure, and electrical properties at interfaces between thin films of titanium and alpha (6H) silicon carbide (0001)*, J. Mater. Res. 10(3), 668-679.
- L.M. Porter, R.F. Davis, J.S.Bow, M.J. Kim, and R.W. Carpenter (1995b), *Chemistry, microstructure, and electrical properties at interfaces between thin films of platinum and alpha (6H) silicon carbide (0001)*, J. Mater. Res. 10(9), 2336-2342
- L.M. Porter, R.F. Davis, J.S. Bow, M.J. Kim, and R.W. Carpenter (1995c), *Chemistry, microstructure, and electrical properties at interfaces thin films of cobalt and alpha (6 H) silicon carbide (0001)*, J. Mater. Res. 10(1), 26-33.

L. Reimer, Ed. (1995), *Energy-Filtering Transmission Electron Microscopy*, Springer Series in Optical Sciences, Springer-Verlag, New York.

J.K. Weiss, R.W. Carpenter, and A.A. Higgs (1991), *A Study of Small Electron Probe Formation in a Field Emission Gun TEM/STEM*, *Ultramicros.* 36, 391-329.

J.K. Weiss, P. Rez and A.A. Higgs (1992), *A computer system for imaging and spectroscopy in analytical electron microscopy*, *Ultramicros.* 41, 291-301.

Handwritten signatures of R.W. Carpenter and S.H. Lin in cursive script.

R.W. CARPENTER and S.H. LIN February 27, 1997.